

Part 6

Winds and the ISM

Section B

Winds

Pulsar Wind Nebulae

James M. Cordes

Astronomy Department, Cornell University, Ithaca, NY 14853

Abstract. I discuss pulsar wind nebulae for which ram pressure from the neutron star's motion is a key element of the morphology. These PWN are tools for determining the pulsar distance, radial velocity component, and interaction of pulsar winds with surrounding media. The Guitar Nebula pulsar (B2224+65) also represents a 'smoking gun' for velocity kicks from asymmetric supernovae or other rocket effects. The detectability of wind nebulae from pulsars and from as-yet unknown neutron stars is discussed.

1. Introduction

Pulsar bowshock nebulae provide rare but distinct opportunities for determining the full three dimensional velocities of pulsars and for analyzing the interactions of pulsar winds with surrounding media. In this paper I survey the known bowshock nebulae, discuss new results on what is probably the most secure high-speed pulsar (the Guitar Nebula pulsar), and address the observability of such nebulae from neutron stars in general.

2. What are Pulsar Wind Nebulae?

Strictly speaking, a large variety of structures may be called pulsar wind nebulae (PWN), for these words may refer to any diffuse object that is visible through an interaction of a pulsar wind with its surroundings. This includes wisps in the Crab Nebula (Arons 1996); X-ray synchrotron nebulae around the Vela pulsar and a few other objects; plerions in general; and bow shock nebulae that I will focus on.

Bow shock nebulae may be distinguished from the 'ghost supernovae' proposed by Blandford *et al.* (1973) as objects surrounding old pulsars. In these 'static PWN', pressure (p_{ism}) from ambient interstellar medium (ISM) and the pulsar wind balance at a radius

$$R_{GS} = \left(\frac{\dot{E}}{4\pi V_A p_{ism}} \right)^{1/2} \sim 2.9 \text{ pc} \left(\frac{\dot{E}_{33}}{p_{-12} V_{A,10}} \right)^{1/2}, \quad (1)$$

where it is assumed that a particle-dominated wind is limited to the Alfvén speed ($V_A = V_{A,10} \times 10 \text{ km s}^{-1}$) through plasma-wave limited flow. GS's of size $\sim 1 \text{ pc}$ for a typical ISM pressure $p_{ism} = p_{-12} \times 10^{-12} \text{ dyne cm}^{-2}$ were sought and not convincingly found.

Bow shocks arise when ram pressure from the neutron star's motion dominates the ambient gas pressure, yielding a cometary-like nebula with pulsar-shock standoff radius

$$R_s = \left(\frac{\dot{E}}{4\pi\rho cV_p^2} \right)^{1/2} \sim 271 \text{ AU} \left(\frac{\dot{E}_{33}}{n_H V_7^2} \right)^2, \quad (2)$$

where V_p is the pulsar's translational speed and it is assumed that the wind is relativistic rather than Alfvén limited. The nominal value is for \dot{E} in units of $10^{33} \text{ erg s}^{-1}$, the pulsar speed in 100 km s^{-1} , and for a hydrogen-only gas with number density n_H . The pairing of relativistic wind flow and ram pressure causes the standoff radius to be much smaller than the radius of ghost nebulae. One advantage of this compactness is that PWN are more easily observable than GS.

The table lists objects that show bow shock nebulae, in order of increasing spin period. The first to be discovered was from the CTB80 (supernova remnant) pulsar B1951+32, followed by the 'black widow' millisecond pulsar (MSP) B1957+20, also seen as an H α nebula. The table indicates that bow shocks have been found around pulsars with a diverse range of spin periods, spindown ages (τ_c), and energy fluxes.

Table 1. Pulsar Wind Nebulae - Bow Shock Short List

Name	P (ms)	τ_c (Myr)	$\log \frac{\dot{E}}{D^2}$ $\left(\frac{\text{erg}}{\text{s kpc}^2} \right)$	V_{\perp}^{\dagger} $\left(\frac{\text{km}}{\text{s}} \right)$	θ_s^{\clubsuit} ($''$)	Reference
B1951+32	39	0.11	35.8	?		1
B1957+20	1.6	1300	34.8	100	4	2
J0437-4715	5.8	900	35.8	89	10	7,8
B1757-24	124	0.29	35.1	?		3
B2224+65	683	1.0	32.5	1729	0.05	4
B1929+10	229	3.0	35.1	71		5,6
B1823-13	101	0.02	35.2	?		9

Notes:

$\dagger V_{\perp}$ is calculated using proper motions and nominal distance.

$\clubsuit \theta_s$ is the shock-pulsar standoff distance in angular units.

References: (1) Hester & Kulkarni 1988; (2) Kulkarni & Hester 1988; (3) Frail & Kulkarni 1991; (4) Cordes, Romani & Lundgren 1993; (5) Yancopoulos, Hamilton & Helfand 1994; (6) Wang, Li & Begelman 1993; (7) Bell *et al.* 1994; (8) Fruchter 1996; (9) Finley *et al.* 1996.

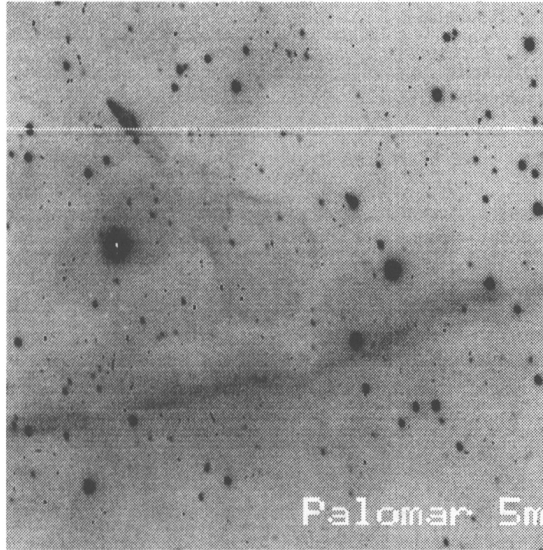


Figure 1. $H\alpha$ image of the Guitar Nebula using the 5m Hale Telescope at Palomar in 1995 August. The length of the nebula is 78 arc sec and the bright patch at the 'neck' is 10.5 arc sec long. The pulsar (at the tip of the bright patch) is moving to the northeast (upward left).

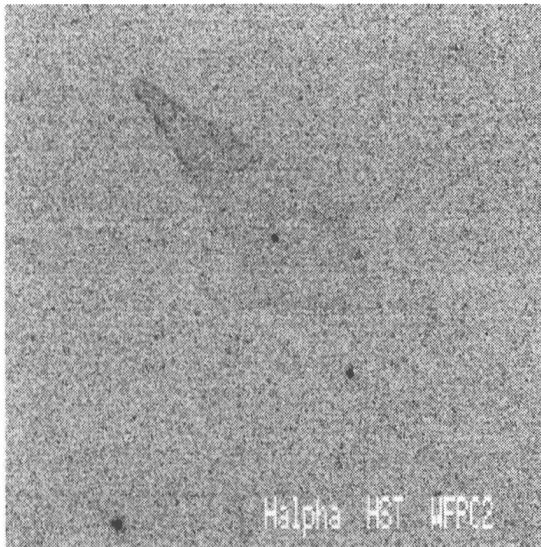


Figure 2. $H\alpha$ image of the bright patch of the Guitar Nebula using the WFPC2 camera on the Hubble Space Telescope in 1994 December. The two stars nearest the $H\alpha$ emission are separated by 5.5 arc sec and are also visible in Figure 1.

3. The Guitar Nebula

One of the most spectacular PWN is the Guitar Nebula, shown in Figures 1 and 2. The pulsar responsible for it is about as ‘garden variety’ as is possible *except* for its large space velocity and, evidently, its partially neutral surroundings. During its lifetime (1 Myr), it has moved 50 deg across the sky. At its nominal distance (Taylor & Cordes 1993), $V_{\perp} \sim 1700 \pm 370 \text{ km s}^{-1}$. The nebula itself shows only $H\alpha$ and $H\beta$ emission, consistent with a nonradiative shock (e.g. Raymond *et al.* 1983). The nebula is undetected at the VLA at 21 and 6 cm and in narrowband IR imaging at Palomar. It is weakly detected in X-rays with the ROSAT/HRI in the guitar body, but not in the vicinity of the pulsar, suggesting detection of shocked interstellar gas at $> 10^6 \text{ K}$. The Palomar image (Figure 1) shows unresolved structure where the pulsar plows into the ISM. Using HST/WFPC2, we resolve the limb-brightened nose of the bow shock (Figure 2). Comparison with Eq. 2 suggests that the true distance may be closer to 1 kpc, though a gas density $n_H < 1 \text{ cm}^{-3}$ could yield consistency at the nominal distance. The X-ray detection favors the nominal distance as well (Romani, private communication). In any case, the distance is not grossly off, so neither is the large transverse speed of 800-1700 km s^{-1} .

The Guitar Nebula pulsar will be monitored and analyzed in the following ways. First, continued mapping of the nebula in $H\alpha$ over 5-10 yr will show changing bowshock contours as the pulsar plows through a changing gas density. Modeling of the nebula should yield its inclination and, hence, the 3D space velocity of pulsar as well as a distance estimate. The dispersion measure should vary at detectable levels, giving additional information about the ambient gas density. The perturbation in DM is $\sim 10^{-3} - 10^{-2} \text{ pc cm}^{-3}$ on time scales $\sim 0.5 \text{ yr}$.

The most important aspect of PSR B2224+65, however, is that it represents a ‘smoking gun’ for velocity kicks. Disruption of a compact binary to produce the estimated *minimum* speed $\sim 800 \text{ km s}^{-1}$ is unlikely, for the required pre-explosion periastron distance is smaller than the size of the progenitor star. Rather, a prompt or delayed rocket effect is required from, respectively, asymmetric energy release during core collapse or asymmetric dipole radiation (Harrison & Tademaru 1975). The existence of B2224+65 therefore corroborates evidence from geodetic spin-axis precession of the Hulse-Taylor binary pulsar (B1913+16) and B1534+12, which require that the systems receive kicks that produce spin-orbit misalignment.

4. Scaling Laws for Bow-shock Emission

Comparison of the bow shocks for two MSPs (J0437-4715 and B1957+20), which have large standoff distances, and the Guitar Nebula, which has a small standoff distance, indicates that Eq. 2 accurately describes the relationship between \dot{E} , V_p and the standoff distance. In general, we may write expressions in terms of observables, taking into account the inclination i of the 3D velocity with respect to the plane of the sky. Letting the 3D velocity be $V_p = V_{\perp} / \cos i = D\dot{\theta}_{\perp} / \cos i$, and the apparent angular offset between a pulsar and the bow shock be $\theta_s =$

$DR_s/\cos i$, we find that

$$\theta_s = \frac{\cos^2 i}{(4\pi\mu_H m_H c)^{1/2}} \left(\frac{\dot{E}/D^2}{n_H V_{\perp}^2} \right)^{1/2}, \quad (3)$$

where μ_H is the mean atomic weight.

The amount of gas swept up is related to the area of the shock nose and, hence, to the standoff radius (Eq. 2) and pulsar velocity. $H\alpha$ photons are produced by collisional excitation of atoms just prior to their ionization in the shock, yielding a line strength

$$F_{\alpha} = (q_{ex}/q_i)n_{HI}V_s\Delta\Omega/4\pi, \quad (4)$$

where $q_{ex}/q_i \approx 0.2$ $H\alpha$ photons are produced per neutral atom and V_s is about equal to the pulsar speed V_p . The solid angle $\Delta\Omega \sim (\eta R_s/D)^2$, where $\eta \sim 30V_7$, with $V_p \equiv 100V_7$ km s⁻¹. In terms of observables and the neutral fraction $X \equiv n_{HI}/n_H$, the $H\alpha$ flux is

$$F_{\alpha} = \frac{10^{-12.8} X n_H V_{\perp}^3 \theta_s^2}{\cos^5 i} = \frac{10^{-2.47} X n_H V_7^3 \theta_s^2 (\text{arc s})}{\cos^5 i} \text{ph cm}^{-2} \text{s}^{-1} \quad (5)$$

The available data on the three $H\alpha$ bow shocks show good consistency with these relations for reasonable values of the hydrogen number density and inclination. More detailed modeling of the bow-shock shape can yield the inclination, distance and constraints on the number density (e.g. Aldcroft *et al.* 1992; Fruchter, 1996).

5. Detectability of Bow Shocks

Because several pulsar bow shocks have been detected in $H\alpha$, it is natural to ask whether additional bow shock nebulae can be found. To see such objects, sufficient neutral gas must be swept up and excited. This requires that, prior to entering the shock, the gas must not be preionized by photons from either the hot neutron star or from shocked gas. A detection criterion based on the flux within a single pixel of a CCD yields a result that is independent of \dot{E}/D^2 . With the Palomar 5m telescope, we obtain (roughly) $n_{HI}V_7/g > 4$ cm⁻³, where g is the attenuation factor due to extinction. More sensibly, a criterion on the total flux within the head of the bow shock (whose size can vary markedly between objects) yields a minimum velocity for the detection of a bow shock that depends on \dot{E}/D^2 :

$$V_{min} = 14 \text{ km s}^{-1} \frac{1}{X\sqrt{n_H}} \left(\frac{\dot{E}_{33}}{D_{kpc}^2} \right)^{-1/2}. \quad (6)$$

Eq. 6 assumes a sensitivity comparable to the Palomar 5m telescope as used in detecting the Guitar Nebula and that the image is optimally smoothed before applying a threshold detection criterion. Pulsars with larger \dot{E}/D^2 or in regions with smaller number density may be slower to allow a PWN detection. However, a smaller neutral fraction, X , increases the required speed.

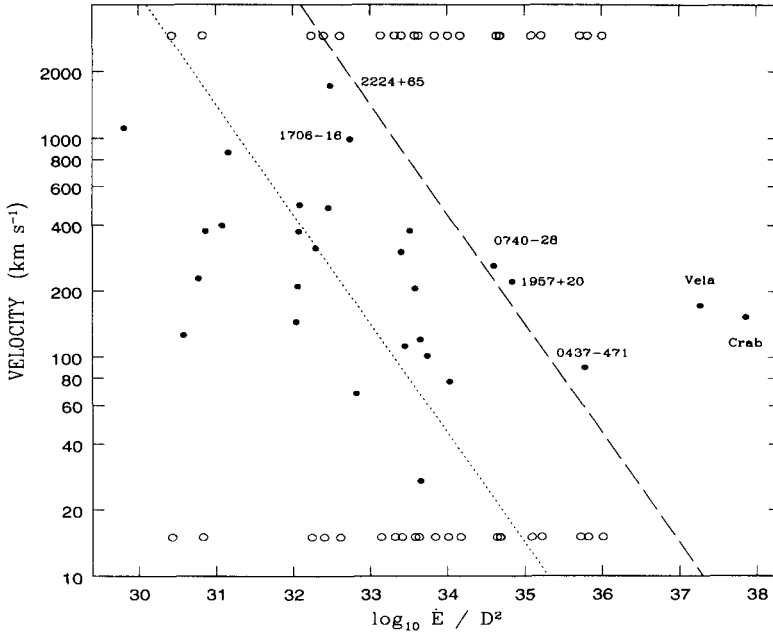


Figure 3. Required space velocity for PWN detection in $H\alpha$ plotted against spindown flux, \dot{E}/D^2 . The lines are the detection criterion of Eq. 6 for $X n_H^{1/2} = 0.01$ (dashed) and 0.1 (dotted). Solid points represent objects that have been observed at Palomar and elsewhere. Open circles represent objects with no measurement of proper motion, plotted at both the top and the bottom of the diagram for comparison with detection criteria. A few objects of interest are labelled. The Crab and Vela pulsars, though well above the plotted detection limits, are not seen as $H\alpha$ nebulae because the neutral fraction is negligible in their vicinities.

Figure 3 shows velocity vs. \dot{E}/D^2 for a subset of known pulsars and two evaluations of Eq. 6, with $X\sqrt{n_H} = 0.01$ (dashed line) and $X\sqrt{n_H} = 0.1$ (dotted line). The figure indicates that for modest number densities and neutral fractions, as are common in the ISM, that the required velocities exceed the mean pulsar velocity ($\sim 400 - 500 \text{ km s}^{-1}$, Lyne & Lorimer 1994) unless \dot{E}/D^2 exceeds $\sim 10^{35} \text{ erg s}^{-1} \text{ kpc}^{-2}$, as it does for the MSPs. The constraint of Eq. 6, combined with the pulsar velocity distribution, and the scale height for neutral gas suggests that bow-shock nebulae are rare objects among the known pulsars, especially when beaming effects are taken into account (Cordes *et al.* 1993). Pulsars not beamed toward us and neutron stars not active as pulsars may be sufficiently large in their numbers to produce bow-shock nebulae that may be detected purposely or serendipitously in H α images.

Acknowledgments. I thank Jon Arons, John Finley, Andy Fruchter, Scott Lundgren & Roger Romani for useful discussions. Scott Lundgren and Roger Romani helped obtain data on the Guitar Nebula. This work was supported by grant AST 92-18075 from the NSF and by the National Astronomy and Ionosphere Center, which operates the Arecibo Observatory under a cooperative agreement with the NSF. Observations at Palomar Observatory were made as part of a collaborative agreement between the California Institute of Technology and Cornell University. Observations with the Hubble Space Telescope were supported by a grant from NASA.

References

- Aldcroft, T.L., Romani, R. W. & Cordes, J.M. 1992, ApJ, 400, 638.
 Arons, J. 1996, these proceedings.
 Bell, J.F. *et al.* 1995, ApJ, 440, 81
 Blandford, R.D. *et al.* 1973, A&A, 23, 145
 Cordes, J.M., Romani, R. W. & Lundgren, S.C. 1993, Nature, 362, 133
 Finley, J.P., Srinivasan, R. & Park, S. 1996, ApJ, submitted
 Frail, D.A. & Kulkarni, S.R. 1991, Nature, 352, 785
 Fruchter, A. 1996, unpublished
 Harrison, T. & Tadamaru, E. 1975, ApJ, 201, 447
 Hester, J.J. & Kulkarni, S.R. 1988, ApJ, 331, L121
 Kulkarni, S.R. & Hester, J.J. 1988, Nature, 335, 801
 Lyne, A.G. & Lorimer, D. 1994, Nature, 369, 127
 Raymond, J.C. *et al.* 1983, ApJ, 275, 636.
 Taylor, J.H. & Cordes, J.M. 1993, ApJ, 411, 674
 Wang, Q.D., Li, Z. & Begelman, M.C. 1993, Nature, 364, 127
 Yancopoulos, S., Hamilton, Y.T. & Helfand, D.J. 1994, ApJ, 429, 832